

Properties of spray deposited nanocrystalline indium selenide thin films

Abhijit A. Yadav¹ · S. D. Salunke²

Received: 2 April 2015 / Accepted: 20 April 2015 / Published online: 29 April 2015
© Springer Science+Business Media New York 2015

Abstract Metal chalcogenide and chalcopyrite thin films have attracted great deal of attention due to their exciting photoelectrical characteristics. Indium selenide thin films have been deposited by computerized chemical spray pyrolysis technique on amorphous glass substrates. The as deposited films are characterized for wide range of properties including structural, surface morphological, optical and electrical, Hall effect and thermo-electrical measurements. X-ray diffraction study revealed that indium selenide thin films are polycrystalline with hexagonal crystal structure irrespective of substrate temperature. Surface morphology and film composition have been analyzed using atomic force microscopy and energy dispersive analysis by X-rays. Nearly stoichiometric deposition of the film at 350 °C was confirmed from EDAX analysis. Optical absorption measurements show that the deposited films possess a direct band gap value of 1.78 eV. The Hall effect study reveals that the films exhibit n-type conductivity.

1 Introduction

World energy demand is continually increasing inexorably in the last ten decades connected to population growth and infinite industrial development. This ever-increasing global energy demand combined with growing concerns about

environmental problems and increasing crude oil prices, illustrate the urgent need for a transition towards alternate renewable energy sources [1–3]. The combination of a technologically advanced modern society and predictions of a future global energy crisis demands the implementation and design of new low-cost, extremely efficient frameworks for solar energy conversion [4, 5]. Today, silicon single crystal based solar cells are dominating the marketplace in the photovoltaic energy field. Nevertheless, semiconductor-compound based devices are also one of the primary topics of solar cell research [6–10]. In order to maintain lower costs, it would be of interest to obtain the photoconductive material in thin film form by using simple and inexpensive technique.

Metal chalcogenide films have attracted significant research attention during the past few decades because of their exciting photoelectrical characteristics. With a general formula of A_2B_3 ; indium selenide is a promising semiconductor material in the applications of solar cells, polymer Schottky diodes, capacitors and batteries, due to its suitable properties. In_2Se_3 belongs to the III–VI compound family. It exhibits many structural modifications and a complicated phase diagram. Also In_2Se_3 (Indium Selenide) is a direct band gap n-type semiconductor having a high absorption coefficient, with potential for utilization in photovoltaic cells and other optoelectronic devices [11–13]. According to previous research, In_2Se_3 has many polymorphic phases, including the layered structure (α -phase), rhombohedral structure (β -phase), defect wurtzite structure (γ -phase) and anisotropic structure (k -phase). The identification of these polymorphs, as well as their crystal structures and physical properties, remain controversial. The controversy arises primarily due to the coexistence of multiple polymorphs in samples, often with similar structures, and sometimes incompletely characterized structures [14, 15].

✉ Abhijit A. Yadav
aay_physics@yahoo.co.in

¹ Thin Film Physics Laboratory, Department of Physics, Electronics and Photonics, Rajarshi Shahu Mahavidyalaya, Latur 413512, Maharashtra, India

² Department of Chemistry and Analytical Chemistry, Rajarshi Shahu Mahavidyalaya, Latur 413512, Maharashtra, India

Generally, the deposition of metal selenide thin films is a challenge to precisely control the grain size, shape and the stoichiometric composition of deposit material. Many groups have contributed to the development of In_2Se_3 thin films by various deposition techniques including vacuum [16], modified chemical bath deposition [17, 18], metal-organic chemical vapor deposition (MOCVD) [19], molecular beam epitaxy [20], sputtering [21, 22], electrodeposition [23, 24], thermal evaporation technique [25, 26], spray pyrolysis [27, 28] etc.

Yan et al. [21, 22] have prepared In_2Se_3 films by magnetron radio-frequency (RF) sputtering technique and subsequently analyzed these films by various characterization techniques. Their analysis showed that γ - In_2Se_3 nanostructures can be successfully grown with a direct band gap 1.94 eV. However, their analysis indicated that film properties strongly depend on the process parameters and there is possibility of using In_2Se_3 thin film in various next-generation photoelectric and optical-memory device applications. Looking forward to Yong Yan et al.'s study, we got motivation and hence tried to study the electrical and optical properties of In_2Se_3 thin films deposited by using a different technique (spray pyrolysis).

A very few reports are available on synthesis of indium selenide thin films by spray pyrolysis. Spray pyrolysis offers a number of advantages, the main ones being its simplicity, capability to produce large areas of highly sensitive films of uniform thickness and the low energy needs for operation. Doping of semiconductor film is simple, since it is accomplished by mere addition of the dopant to the spray solution [29, 30]. Considering all these aspects efforts have been made to deposit indium selenide thin films at different substrate temperatures and additionally its effect on optical, compositional and electrical properties has been studied.

2 Experimental details

Indium selenide thin films are deposited onto glass substrates by a computerized spray pyrolysis method [31]. The substrate temperature was varied from 300 to 400 °C at the interval of 25 °C. Aqueous solutions equimolar (0.05 M) of Indium chloride (InCl_3) and selenourea ($\text{H}_2\text{NC}(\text{Se})\text{NH}_2$) were used as starting materials in the ratio 2:3. Well cleaned glass microslides of the size $7.5 \times 2.5 \text{ cm}^2$ were used as substrates. The various preparative parameters used were optimized with photoelectrochemical (PEC) techniques. The substrate temperature was controlled by an iron–constantan thermocouple. A spray rate employed was of $3\text{--}4 \text{ cc min}^{-1}$. The nozzle to substrate distance was 28 cm. After deposition, the films were allowed to cool at

room temperature. The adhesion of the films onto the substrate was quite good.

The as deposited indium selenide thin films at different substrate temperatures were characterized for structural, morphological, compositional, optical, electrical, thermo-electric properties and Hall effect measurements. The film thickness of the as-deposited films was measured by a well known gravimetric weight difference method using sensitive microbalance and assuming bulk density of In_2Se_3 . The structural characterization of the films was carried out by using Philips PW-3710 X-ray diffractometer with Cu-K_α radiation, within the 2θ range of angles between 10° and 80°. Atomic force microscopy (AFM) was carried out to study surface morphology in air at ambient condition (300 K) using Nanoscope III from Veeco. A UV–Vis spectrophotometer (SHIMADZU UV-1700) was used to record the optical absorption spectra of the samples in the wavelength range 350–850 nm. Electrical resistivity and thermo electric power measurements were done using D.C. two point probe method. Hall effect setup supplied by Scientific Equipments, Roorkee, India was used for measurements of electrical parameters like carrier concentration (n) and mobility (μ) at room temperature. Vander Pauw technique [32] was used for this.

3 Results and discussion

3.1 Growth mechanism

The variation in film thickness with substrate temperature for spray deposited indium selenide thin films is shown in Fig. 1; relatively higher thickness of 650 nm was observed for film deposited at 350 °C. It reflects that the film thickness increases with increasing substrate temperature from 300 to 350 °C, attain maximum value at 350 °C (650 nm), beyond that it decreases. This behavior can be explained as follows: Initially, at lower substrate temperatures e.g., 300 °C, the temperature may not be sufficient to decompose the sprayed droplets of In^{3+} and Se^{2-} ions from the solution and this result in a lower thickness. At a particular substrate temperature 350 °C, decomposition occurs at the optimum rate resulting in terminal thickness. A noticeable decrease of the film thickness with increasing the substrate temperature is observed after 350 °C. This decrease may be attributed to re-evaporation of film material after deposition or to thermal convection of the sprayed droplet during the deposition process or both. Another cause which may account for thickness decrease is water loss or removal of interlayer water with consequent formation of the compact film [33]. The thickness values for films at various substrate temperatures are given in Table 1.

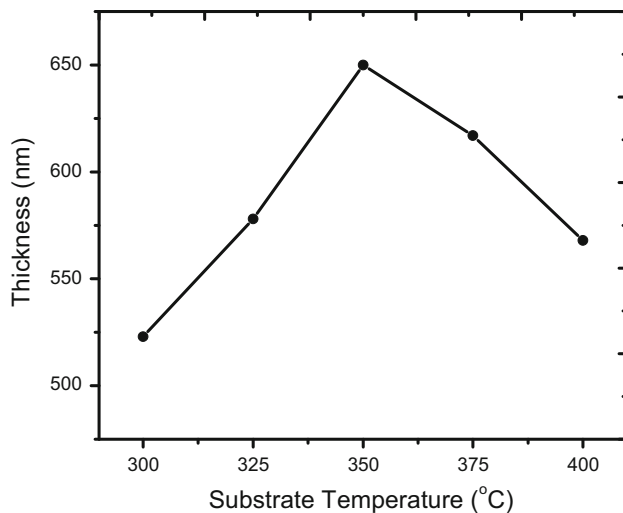
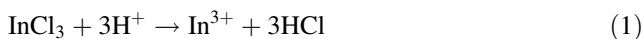


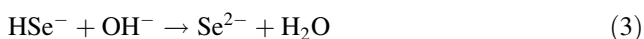
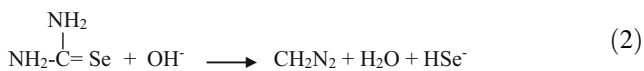
Fig. 1 Plot of film thickness versus substrate temperature for spray deposited indium selenide thin films

A simple reaction mechanism for deposition of indium selenide thin films can be written as follows:

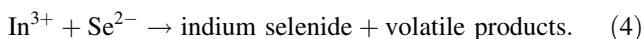
In the present case, In^{3+} ions are released into by the dissociation equilibria presented by;



The selenide ions are released due decomposition of selenourea as,



In presence of metal indium ions the reaction will be,



3.2 Structural studies

The crystal structure of indium selenide thin films was studied by X-ray diffraction with Cu-K_α radiation (1.5406 Å). Figure 2 shows X-ray diffraction patterns of indium selenide film deposited at various substrate temperatures. It was observed that the high intensity reflection peaks occur at $2\theta = 25.66^\circ$ (1 0 0) plane, $2\theta = 27.26^\circ$ (1 0 1) plane, $2\theta = 31.70^\circ$ (1 0 2) plane and $2\theta = 45.34^\circ$ (1 1 0) plane for In_2Se_3 thin film which indicates that the growth of the thin films occurred preferentially in the direction perpendicular to the sample's surface. All peaks match to the standard indium selenide pattern fairly well, indicating a polycrystalline hexagonal crystal structure without any noticeable secondary phases. It is also easy to

Table 1 Values of thickness, crystallite size and surface roughness for spray deposited In_2Se_3 thin films

Substrate temperature (°C)	Thickness (nm)	Crystallite size (nm)	Surface roughness (RMS value) (nm)
300	523	18	7.09
325	578	21	4.73
350	650	26	2.85
375	617	24	3.67
400	568	22	4.12

see that despite the difference in substrate temperature the all films exhibit a preferred (1 0 2) orientation, with nearly matching XRD patterns [34].

No peaks correspond to oxide phases, which demonstrates that the $[\text{Se}]/[\text{In}]$ ratio (2:3) we employed avoided formation of undesirable oxide phases. This finding is supported by the absence of any oxide-related diffraction peaks. The intensity of main peak (1 0 2) produced by In_2Se_3 thin film increased with the substrate temperature up to 350 °C, but it decreased slightly after 350 °C. Therefore, the film deposited at 350 °C had the highest intensity and it exhibited better crystallization. Initially, there were many crystallites present in the as-deposited films that exhibited less intense peaks and when the layers were deposited at a particular substrate temperature (350 °C) the small crystallites grew into larger ones with an improved crystallinity. The observed structural changes were attributed to the coalescence induced grain growth during high temperature deposition process where smaller nuclei could easily rotate compared to the larger nuclei in order to minimize the interfacial energy. At optimum substrate temperatures, the atoms have sufficient thermal energy to move into stable positions, so that structural reorientation occurs, leading to a significant increase in the intensity of (1 0 2) plane. Extended crystalline phases represent a prerequisite in photovoltaic applications [35]. After refinement, the cell constants were calculated to be $a = b = 4.014 \text{ \AA}$ and $c = 9.64 \text{ \AA}$; which are consistent with the reported data [36].

The effect of substrate temperature on the orientation of polycrystalline In_2Se_3 thin films was investigated by evaluating the texture coefficient ($T_c(hkl)$) of the (hkl) plane using the formula given by Klug and Alexander [37],

$$T_c(hkl) = \frac{I(hkl)/I_0(hkl)}{(1/N) \left(\sum_N I(hkl)/I_0(hkl) \right)} \quad (5)$$

where $T_c(hkl)$ is the texture coefficient of the (hkl) plane, I is the measured intensity and I_0 is the JCPDS standard intensity, N is the number of diffraction peaks. From the above Eq. (5), it is seen that the value of texture coefficient

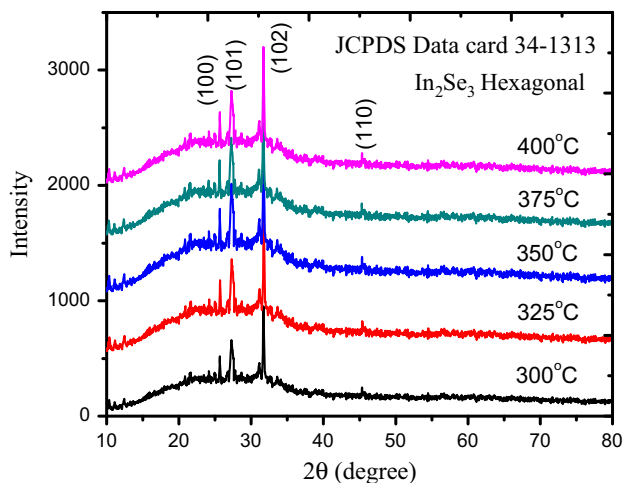


Fig. 2 X-ray Diffraction patterns of indium selenide thin films deposited at various substrate temperatures

approaches unity for a randomly distributed powder sample, while $T_c(hkl)$ is greater than unity when the (hkl) plane is preferentially oriented.

Figure 3 shows the variation of texture coefficient for (1 0 2) plane with respect to substrate temperature of polycrystalline In_2Se_3 thin films. From Fig. 3; it is clear that the lower value of texture coefficient represents that the films have poor crystallinity and the crystallinity is found to be improved by increasing substrate temperature from 300 to 350 °C. Further increase in substrate temperature above 350 °C, the value of texture coefficient slightly decreases. Hence, it is concluded that In_2Se_3 thin films obtained at 350 °C have better crystallinity as well as better adherence to the substrates.

Crystallite size was estimated by using Scherrer’s formula given by the equation;

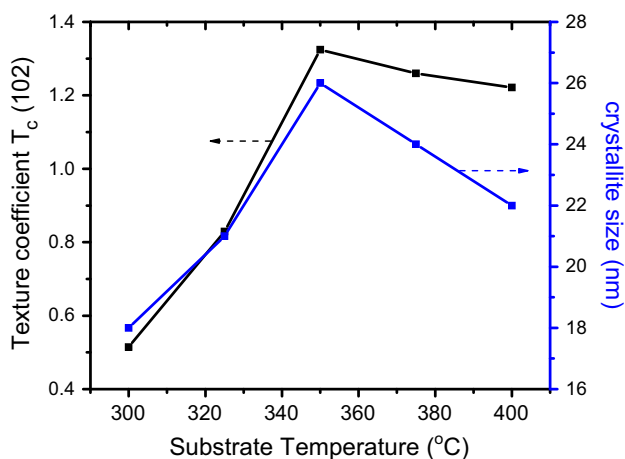


Fig. 3 Plot of texture coefficient (T_c) and crystallite size versus substrate temperature for spray deposited indium selenide thin films

$$D = \frac{k\lambda}{\beta \cdot \cos \theta} \tag{6}$$

where k varies from 0.89 to 1.39. But in most of the cases it is closer to 1. Hence for grain size calculation it is taken to be one, λ is wavelength of X-ray, β is the full width at half of the peak maximum in radians and θ is Bragg’s angle. The crystallite size was estimated for the standard (1 0 2) reflection. The crystallite size for indium selenide thin films was found to be in the range of 18–26 nm. The crystallite size increases with temperature up to 350 °C (reaching a maximum of 26 nm), followed by a slight decrease, with further increase in the substrate temperature. However, higher temperatures may yield lattice stress, defects formation and increases non-stoichiometry. The values crystallite sizes are plotted in Fig. 3.

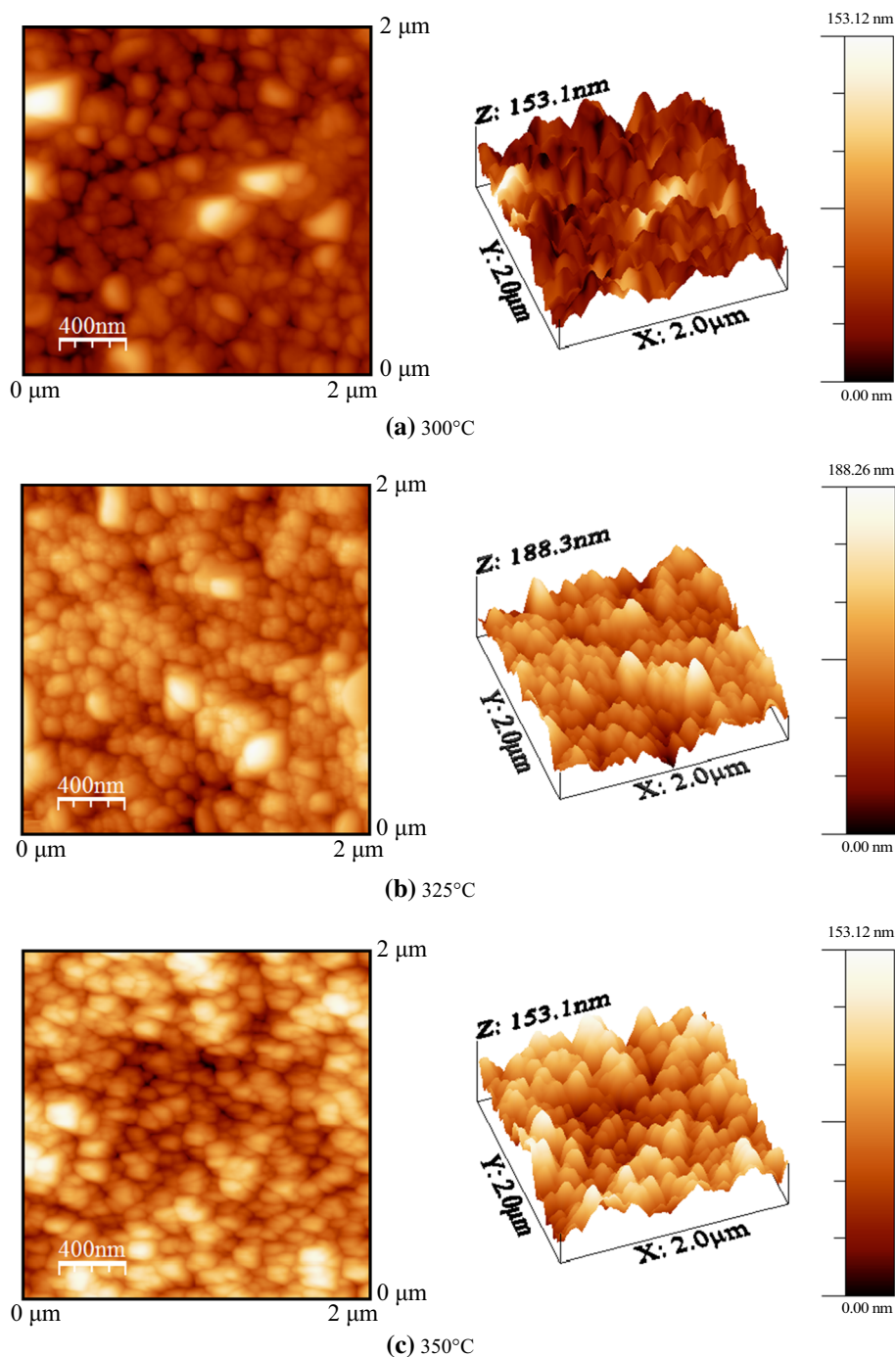
3.3 Surface morphological and compositional studies

The surface morphology of indium selenide thin films was investigated using AFM technique. AFM is a well known characterization technique commonly used to study surface morphology with very high, sometimes even molecular or atomic resolution. The AFM system used in these studies is the Nanoscope III multimode scanning probe microscope, produced by the Digital Instruments, Veeco Metrology Group, USA. The detailed analysis of all obtained AFM data was performed with the help of the WSxM 4.0 (Nanotec electronica S.L.) software. This software allows us to extract the basic topographic information. The surface morphology was studied by AFM; root mean square (RMS) roughness of the films was extracted from AFM data.

Figure 4(a–e), shows typical two-dimensional (2D) and three-dimensional (3D) AFM images of $2.0 \times 2.0 \mu m^2$ size of the indium selenide thin film deposited at various substrate temperatures. The AFM micrographs (Fig. 4a–e) show that the films adhered well to the substrate, compact, and homogeneous, thereby making them suitable for photovoltaic applications, with a small grain size, particularly the samples produced at 350 °C. The sample roughness measurements indicate that the sample deposited at a low substrate temperature (300 °C) was rougher than the others, which can be explained by the segregation of small grains to form irregular large grains with boundaries. Table 1 shows the surface roughness measurements obtained by AFM. The surface roughness is unavoidable due to three-dimensional growth of the film [38, 39].

The quantitative analysis of the films was carried out by using the EDAX technique for the as-deposited films at different substrate temperatures to study the stoichiometry of the indium selenide films. Figure 5 shows the typical

Fig. 4 Two-dimensional (2D) and three-dimensional (3D) AFM images of indium selenide thin films deposited at various substrate temperatures



EDAX pattern for spray deposited indium selenide thin film at a substrate temperature of 350 °C. The elemental analysis was carried out only for In and Se; the average atomic percentage of In: Se was 37.03:62.97. It is close to 2:3 for as-deposited In_2Se_3 film at 350 °C. Similar results for In_2Se_3 were reported by Afzaal et al. [40] using EDAX. Table 2 Shows the compositional analysis of spray deposited In_2Se_3 thin films at different substrate temperatures.

3.4 Optical studies

The optical absorption spectra of the sprayed In_2Se_3 films grown at various substrate temperatures were studied by using UV–Vis spectrophotometer (SHIMADZU UV-1700) in the wavelength range 350–850 nm. All the films have comparable absorbance in the visible spectral range and initially the absorbance increases with substrate temperature up to 350 °C decreases thereafter for further increase in

Fig. 4 continued

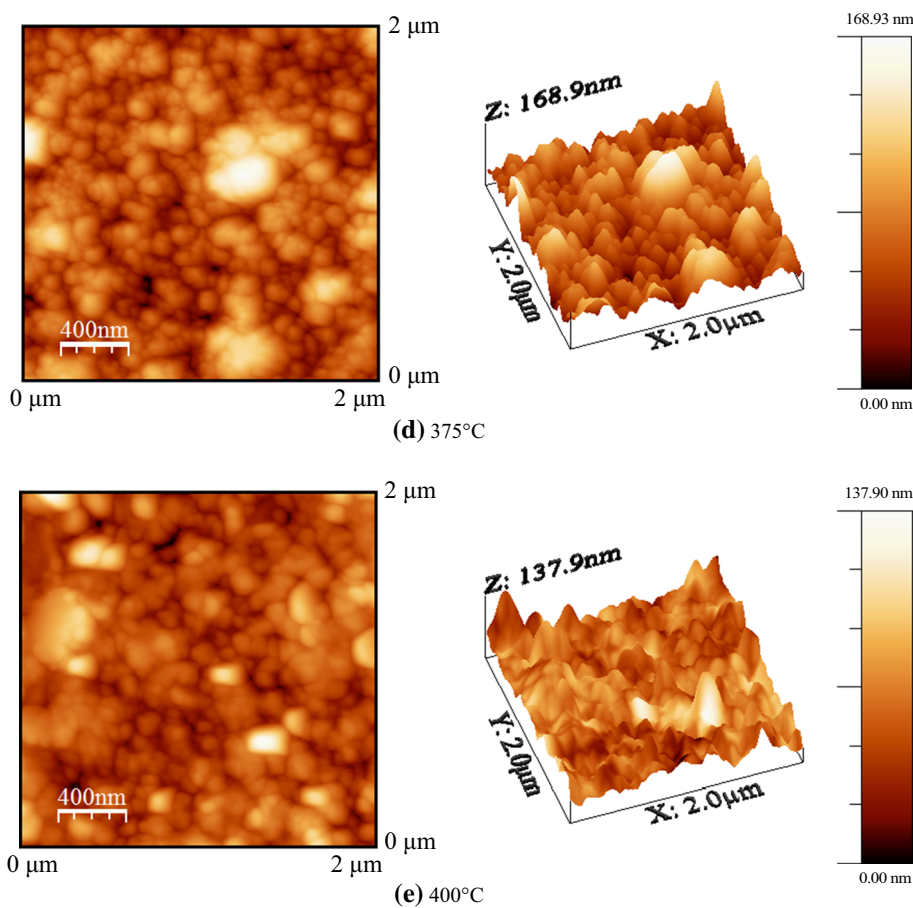
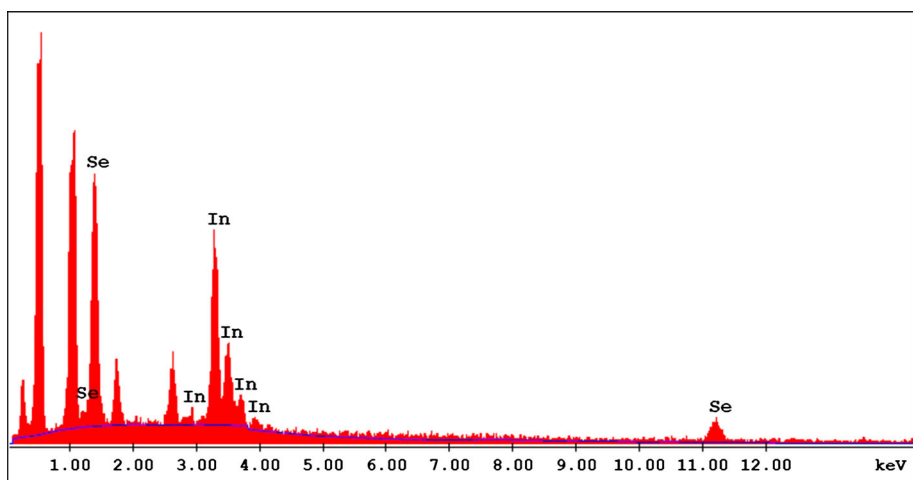


Fig. 5 EDAX spectrum of indium selenide thin films deposited at a substrate temperature 350 °C



temperature. This can be explained by the slight decrease in the thickness of the films deposited at higher temperatures as result of the densification process, forming larger grains [35, 41]. The absorbance significantly decreases in the IR spectral range (beneficial fact in the photovoltaic conversion), proving that these optical parameters are morphology-related, and could be corroborated with the multiple scattering

on the small-sized grains that lead to a more efficient radiation trapping in UV and Vis [42].

The absorption coefficient, optical band gap and type of transition involved were determined from the absorption data. The value of absorption coefficient is found to be of the order of 10^4 cm^{-1} . The optical band gap (E_g) values were determined from the commonly known equation:

Table 2 Compositional analysis and electrical properties of spray deposited In₂Se₃ thin films at various substrate temperatures

Substrate temperature (°C)	Atomic percentage		Room temperature Resistivity ρ	Carrier concentration(n)	Mobility (μ)
	In	Se	(Ω -cm) $\times 10^4$	$\times 10^{16} \text{ cm}^{-3}$	$\times 10^{-3} \text{ cm}^2 \text{ V}^{-1} \text{ s}^{-1}$
300	36.17	63.83	2.79	5.14	4.53
325	36.96	63.04	4.35	7.02	6.58
350	37.03	62.97	0.53	8.27	14.4
375	36.99	63.01	0.88	7.65	9.29
400	36.48	63.52	1.55	7.57	5.32

$$\alpha hv = A(hv - E_g)^n \quad (7)$$

where A is a constant related to the effective masses of charge carriers, h is the Planck constant, E_g is the band gap energy, $h\nu$ is the incident photon energy, and n is the exponent that depends on the nature of the optical transition ($n = 2$ or $1/2$ for indirect or direct transition respectively). The optical band gaps of the indium selenide thin films deposited at various substrate temperatures were evaluated based on the linear form of Eq. (7), Fig. 6a. The plot of $(\alpha h\nu)^2$ versus $(h\nu)$ for spray deposited indium selenide thin film at different substrate temperatures is linear at the absorption edge, indicating a direct allowed transitions. The straight line portion was extrapolated to the energy axis and when $(\alpha h\nu)^2 = 0$, the intercept gives the bandgap energy of In₂Se₃. The band gap values (1.78–1.98 eV) are in good agreement with the values obtained by other researchers [43] and the temperature effect on E_g confirms recent reports [44]. The variation of bandgap energy E_g with the substrate temperature depicted in Fig. 6b. It is found that bandgap energy E_g decreases with a substrate temperature reaches a minimum value 1.78 eV at 350 °C and further increases with increase in substrate temperature. The variation in the E_g values could be correlated with (a) the reduction of the density of band tail states, i.e. reduced localized disordered regions in the bandgap and/or (b) significant deviations from stoichiometry of the In₂Se₃ compound as observed from EDAX and smaller grain sizes [45]. These results suggest that the optical band gap of In₂Se₃ thin films can be controlled more precisely by controlling the substrate temperatures.

3.5 Electrical and thermo electrical studies

The temperature dependence electrical resistivity of spray deposited In₂Se₃ thin films was studied in the temperature range of 300–500 K. The variation of log (resistivity) with reciprocal of temperature for a cooling cycle of spray

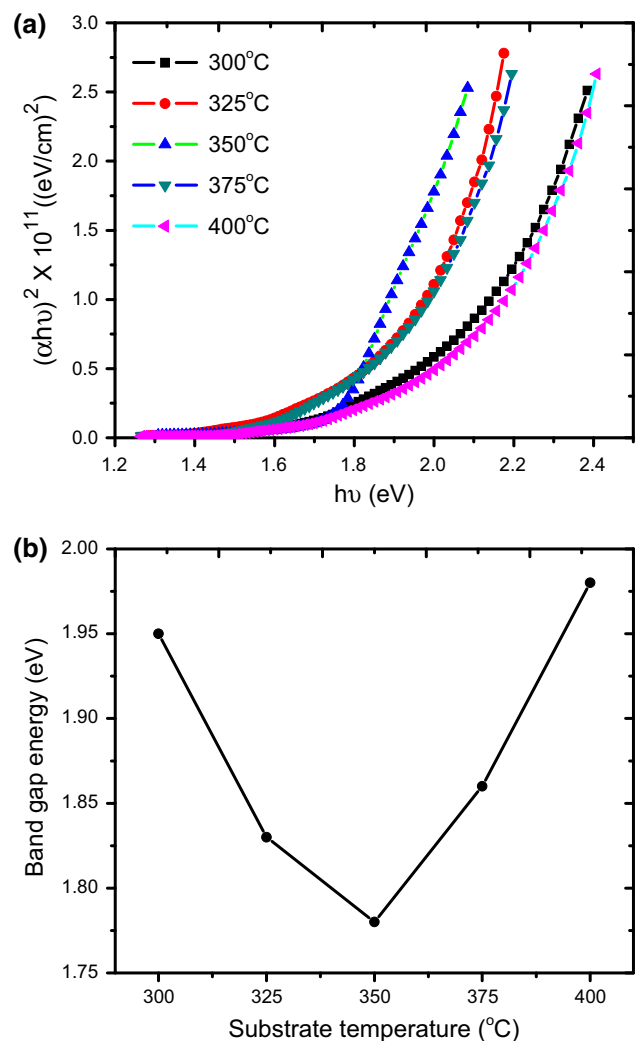


Fig. 6 Plot of **a** $(\alpha h\nu)^2$ versus $h\nu$ of indium selenide thin films deposited at various substrate temperatures and **b** bandgap energy versus substrate temperature for indium selenide thin films

deposited indium selenide thin films at various substrate temperatures is shown in Fig. 7. It shows that spray deposited indium selenide film is semiconducting and

nonlinear nature of the plots shows the presence of many defect levels in the films. The room temperature electrical resistivity of the indium selenide thin films is found to be $2.79 \times 10^4 \Omega\text{-cm}$ for film deposited at 300 °C substrate temperature, which decreases to $0.53 \times 10^4 \Omega\text{-cm}$ for film deposited at 350 °C substrate temperature, and further increases with increase in substrate temperature. The initial decrement in resistivity with substrate temperature may be associated with crystallite size of developed film. It was observed from XRD data that with increase in the substrate temperature of the film from 300 to 350 °C, crystallite size of developed film increases. As a result of this, inter crystalline barrier decreases, and hence charge carriers have to cross minimum number of crystalline boundaries during the electrical charge flow. Therefore, resistivity decreases. However, it was also found that for substrate temperature greater than 350 °C, crystallite size somewhat decreases, which causes the appearance of more number of crystalline boundaries. As a result of this, charge carriers have to face maximum number of grain boundaries during charge flow, hence resistivity increases. The resistivity results of the thin films are consistent with other studies [24, 26].

The values of activation energies (E_a) were determined by Arrhenius equation given by [46]

$$\rho = \rho_0 \exp \frac{E_a}{kT} \tag{8}$$

where ρ and ρ_0 electrical resistivity's, k is the Boltzmann constant and T is the absolute temperature. From Fig. 7 the variation indicated two distinct temperature zones with two characteristic regions. The first region from room temperature up to 370 K is identified with low temperature and extends upwards as far as the impurity exhaustion

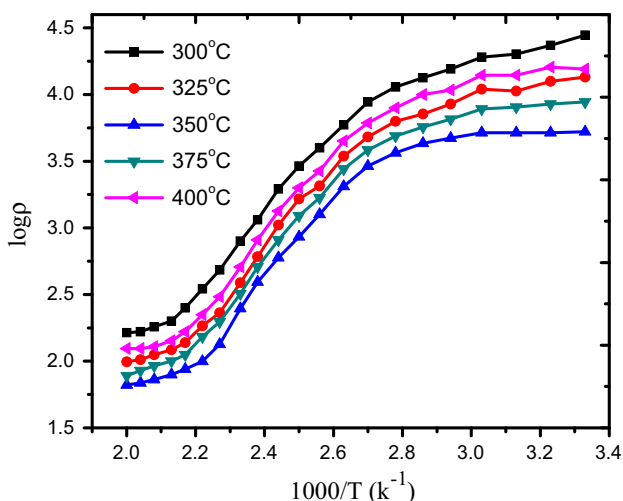


Fig. 7 Plot of $\log \rho$ versus inverse of absolute temperature for indium selenide thin films deposited at various substrate temperatures

temperatures. This region is identified with the extrinsic conductivity of semiconductor due to the ionization of impurity atoms. The second region from 370 up to 500 K is identified with the transition to intrinsic conduction in semiconductor. Within this region, the density of carriers is equal to that of intrinsic carriers. The E_a is found to be in the range between 1.07 and 7.59 meV in the low temperature region and 10.6–18.2 meV in the high temperature region. The values of the activation energy indicate that the prepared samples are semiconductors. Similar results were obtained by Bindu et al. [47] for chemically deposited In_2Se_3 thin films.

The type of conductivity exhibited by the spray deposited In_2Se_3 thin films is determined from TEP measurement. Figure 8 shows variation of thermoemf with temperature difference (T) for spray deposited indium selenide thin film deposited at various substrate temperatures. The polarity of thermo-emf was positive towards hot end with respect to cold end, which confirms the fact that In_2Se_3 films are of n-type. The thermoemf is of the order of mV.

3.6 Hall effect analysis

From the Hall effect measurements, the positive polarity of Hall coefficient, it was evident that the as-deposited indium selenide films are n-type semiconductor. The variation of film carrier concentration (n) and room temperature mobility (μ) plotted against substrate temperatures shown in Fig. 9. Carrier concentration increases with a substrate temperature up to 350 °C and decreases thereafter. The increase carrier concentration observed at 350 °C can be related to both the observed improvement in crystallinity of the indium selenide thin films without any residual amorphous content and to a pin hole free surface due to the fact

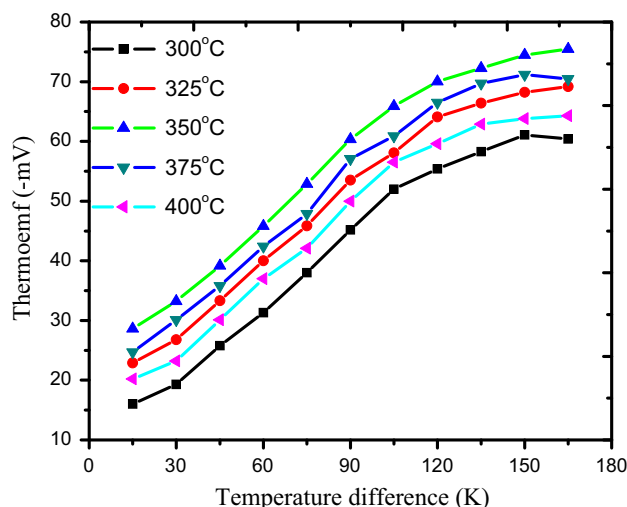


Fig. 8 Plot of thermo-emf versus temperature difference for the indium selenide thin films deposited at various substrate temperatures

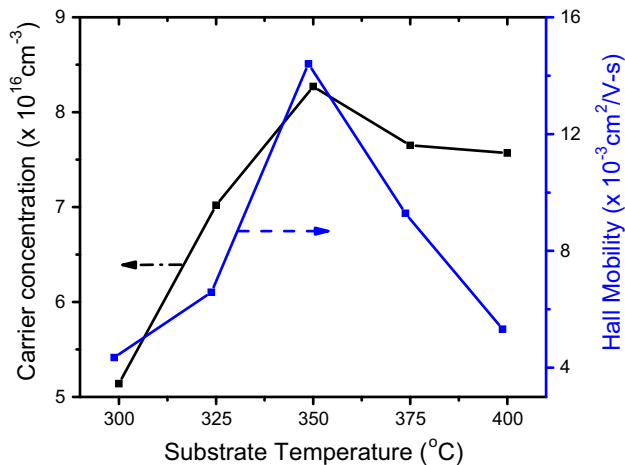


Fig. 9 Plot of carrier concentration (n) and Hall mobility (μ) versus substrate temperature for spray deposited indium selenide thin films

that these films grown at the optimal temperature mediated a CVD process. The values of carrier concentration and mobility for the film deposited at 350 °C are $8.27 \times 10^{16} \text{ cm}^{-3}$ and $14.4 \times 10^{-3} \text{ cm}^2 \text{ V}^{-1} \text{ s}^{-1}$; respectively with n-type conductivity. The values of carrier concentration and mobility for indium selenide thin films deposited at various substrate temperatures are given in Table 2 and are in good agreement with reported data [48, 49].

4 Conclusions

In_2Se_3 thin films can be deposited by chemical spray pyrolysis technique. Polycrystalline nature with hexagonal crystal structure was revealed for all compositions from X-ray diffraction studies. Films with crystallite size in the range of 18–26 nm can be obtained. The surface morphology of the material is uniform. EDAX study confirmed nearly stoichiometric deposition of In_2Se_3 thin films. The absorbance significantly decreases in the IR spectral range (beneficial fact in the photovoltaic conversion), proving that these optical parameters are morphology-related, and could be corroborated with the multiple scattering on the small-sized grains that lead to a more efficient radiation trapping in UV and Vis. The absorption spectra of these composites showed a high coefficient of absorption with direct allowed type of optical transitions with band gap of 1.78 eV. All films are semiconducting in nature with n-type conductivity. Finally it is concluded that the improvement in the crystalline nature and decrease in the optical band gap are important physical properties of the material that can play a crucial role for effective harnessing the solar energy.

Acknowledgments Dr. A. A. Yadav is grateful to the Science and Engineering Research Board, Department of Science and Technology, New Delhi, India for the financial assistance through the Project under SERC Fast Track Scheme for Young Scientist (File No. SB/FTP/PS-068/2013).

References

1. A.A. Yadav, J. Mater. Sci. Mater. Electron. **25**, 3096 (2014)
2. M. Emziane, S. Marsillac, J.C. Bernede, Mater. Chem. Phys. **62**, 84 (2000)
3. A.A. Yadav, E.U. Masumdar, Sol. Energy **84**, 1445 (2010)
4. A.A. Yadav, E.U. Masumdar, J. Alloys Compd. **509**, 5394 (2011)
5. A.A. Yadav, E.U. Masumdar, Electrochim. Acta **56**, 6406 (2011)
6. M.L. Gaur, P.P. Hankare, K.M. Garadkar, S.D. Delekar, V.M. Bhuse, J. Mater. Sci. Mater. Electron. **25**, 190 (2014)
7. M.R. Asabe, V.P. Ubale, A.H. Manikshete, V.T. Vader, S.V. Rajmane, S.D. Delekar, J. Mater. Sci. Mater. Electron. **24**, 4655 (2013)
8. A.A. Yadav, M.A. Barote, E.U. Masumdar, Sol. Energy **84**, 763 (2010)
9. M.J. Deen, F. Pascal, J. Mater. Sci. Mater. Electron. **17**, 549 (2006)
10. H.-B. Xie, W.-F. Liu, X.-Y. Li, F. Yan, G.-S. Jiang, C.-F. Zhu, J. Mater. Sci. Mater. Electron. **24**, 475 (2013)
11. S. Yang, D.F. Kelly, J. Phys. Chem. B **109**, 12701 (2005)
12. J. Han, C. Liao, T. Jiang, H. Xie, K. Zhao, M.-P. Besland, J. Mater. Sci. Mater. Electron. **25**, 2237 (2014)
13. J. Wang, J. Zhu, L.-L. Liao, J. Mater. Sci. Mater. Electron. **25**, 1863 (2014)
14. P.P. Hankare, K.C. Rathod, M.R. Asabe, A.V. Jadhav, V.B. Helavi, S.S. Chavan, K.M. Garadkar, I.S. Mulla, J. Mater. Sci. Mater. Electron. **24**, 2398 (2013)
15. T. Zhai, X. Fang, M. Liao, X. Xu, L. Li, B. Liu, Y. Koide, Y. Ma, J. Yao, Y. Bando, D. Golberg, ACS Nano **4**, 1596 (2010)
16. J.P. Guesdon, B. Kobbli, C. Julien, M. Balkanski, Phys. Status Solidi A **102**, 327 (1987)
17. P.P. Hankare, M.R. Asabe, P.A. Chate, K.C. Rathod, J. Mater. Sci. Mater. Electron. **19**, 1252 (2008)
18. M.R. Asabe, P.A. Chate, S.D. Delekar, K.M. Garadkar, I.S. Mulla, P.P. Hankare, J. Phys. Chem. Solids **69**, 249 (2008)
19. D.Y. Lyu, T.Y. Lin, T.W. Chang, S.M. Lan, T.N. Yang, C.C. Chiang, C.L. Chen, H.P. Chiang, J. Alloys Compd. **499**, 104 (2010)
20. T. Okamoto, A. Yamada, M. Konagai, J. Cryst. Growth **175**(176), 1045 (1997)
21. Y. Yan, S. Li, Y. Zhou, L. Liu, C. Yan, Y. Zhang, Y. Zhao, Opt. Mater. **38**, 217 (2014)
22. Y. Yan, S. Li, O. Yufeng, Y. Ji, L. Liu, C. Yan, Y. Zhang, Y. Zhou, Y. Zhao, J. Alloys Compd. **614**, 368 (2014)
23. S. Ikeda, R. Kamai, S.M. Lee, T. Yagi, T. Harada, M. Matsumura, Sol. Energy Mater. Sol. Cells **95**, 1446 (2011)
24. M.L. Madugu, L. Bowen, O.K. Echendu, I.M. Dharmadasa, J. Mater. Sci. Mater. Electron. **25**, 3977 (2014)
25. M.A. Afifi, N.A. Hegab, A.E. Bekheet, Vacuum **46**, 335 (1995)
26. S.S. Sen, N.N. Biswas, K.A. Khan, Appl. Energy **65**, 51 (2000)
27. J. George, K.S. Joseph, T.I. Palson, Phys. Status Solidi A **106**, 123 (1988)
28. A.A. Yadav, J. Alloys Compd. (2015). doi:10.1016/j.jallcom.2015.04.041
29. H. Bouzouita, N. Bouguila, S. Duchemin, S. Fiechter, A. Dhouib, Renew. Energy **25**, 131 (2002)
30. W.-T. Kim, C.-D. Kim, J. Appl. Phys. **60**, 2631 (1986)

31. A.A. Yadav, M.A. Barote, P.M. Dongre, E.U. Masumdar, J. Alloys Compd. **493**, 179 (2010)
32. L.J. Van der Pauw, Philips Res. Rep. **13**, 1 (1958)
33. A.A. Yadav, J. Mater. Sci. Mater. Electron. **25**, 1251 (2014)
34. JCPDS Data card 34-1313
35. M. Baneto, A. Enesca, C. Mihoreanu, Y. Lare, K. Jondo, K. Napo, A. Duta, Ceram. Int. **41**, 4742 (2015)
36. K.J. Chang, S.M. Lahn, Z.J. Xie, J.Y. Chang, W.Y. Uen, T.U. Lu, J.H. Lin, T.Y. Lin, J. Crys. Growth **306**, 283 (2007)
37. H.P. Klug, L.E. Alexander, *X-Ray Diffraction Procedures* (Wiley, New York, 1954)
38. A.A. Yadav, J. Alloys Compd. **552**, 318 (2013)
39. A.A. Yadav, J. Alloys Compd. **543**, 129 (2012)
40. M. Afzaal, D. Crouch, P. O'Brien, Mater. Sci. Eng. B **116**, 391 (2005)
41. S.M. Wu, Y.Z. Xue, L.M. Zhou, X. Liu, D.Y. Xu, J. Alloys Compd. **600**, 96 (2014)
42. Z. Peng, Y. Liu, W. Shu, K. Chen, W. Chen, Chem. Phys. Lett. **586**, 85 (2013)
43. S. Marsillac, A.M. Combat-Marie, J.C. Bernede, A. Conan, Thin Solid Films **288**, 20 (1996)
44. S.W. Shin, J.H. Han, J.Y. Lee, Y.C. Park, G.L. Agawane, A.V. Moholkar, M.G. Gang, C.H. Jeong, J.H. Kim, J.H. Yun, Appl. Surf. Sci. **270**, 572 (2013)
45. A.A. Yadav, M.A. Barote, E.U. Masumdar, Mater. Chem. Phys. **121**, 53 (2010)
46. K.J. Laidler, *The World of Physical Chemistry* (Oxford University Press, Oxford, 1993)
47. K. Bindu, C. Sudha Kartha, K.P. Vijaykumar, T. Abe, Y. Kashiwala, Appl. Surf. Sci. **191**, 138 (2002)
48. C. Julien, M. Eddrief, K. Kambas, M. Balkanski, Thin Solid Films **137**, 27 (1986)
49. D. Manno, G. Micocci, R. Rella, P. Siciliano, A. Tepore, Vacuum **46**, 997 (1995)